Research article

JHEP|Reports

Downregulation of hepatic METTL3 contributes to APAP-induced liver injury in mice

Chunhong Liu,[1,†] **Xinzhi Li**,[1,†] Ming Gao,[1] Yanbin Dong,[2] Zheng Chen[1,*]

[1]*HIT Center for Life Sciences, School of Life Science and Technology, Harbin Institute of Technology, Harbin 150001, China;* [2]*Institute of Biophysics, Chinese Academy of Sciences, Beijing, China*

JHEP Reports **2023.** https://doi.org/10.1016/j.jhepr.2023.100766

Background & Aims: Acetaminophen (APAP) overdose is a major cause of acute liver failure in the Western world, but its molecular mechanisms are not fully understood. Methyltransferase-like 3 (METTL3) is a core N6-methyl-adenosine (m6A) RNA methyltransferase that has been shown to regulate many physiological and pathological processes. This study aimed to investigate the role of METTL3 in APAP-induced liver injury in mice.

Methods: Hepatocyte-specific *Mettl3* knockout (*Mettl3*-HKO) mice and adenovirus-mediated gene overexpression or knockdown were used. We assayed APAP-induced liver injury by measuring serum alanine aminotransferase/aspartate aminotransferase activity, necrotic area, cell death, reactive oxygen species levels and activation of signalling pathways. We also performed mechanistic studies using a variety of assays and molecular techniques.

Results: Hepatic METTL3 is downregulated in APAP-induced liver injury, and hepatocyte-specific deletion of *Mettl3* accelerates APAP-induced liver injury, leading to increased mortality as a result of the dramatic activation of the mitogen-activated protein kinase kinase 4 (MKK4) / c-Jun NH2-terminal kinase (JNK) signalling pathway. Inhibition of JNK by SP600125 largely blocks APAP-induced liver injury in *Mettl3*-HKO mice. Hepatic deletion of *Mettl3* activates the MKK4/JNK signalling pathway by increasing the protein stability of MKK4 and JNK1/2 as a result of decreased proteasome activity. Restoration of proteasome activity by overexpression of proteasome 20S subunit beta 4 (PSMB4) or proteasome 20S subunit beta 6 (PSMB6) leads to the downregulation of MKK4 and JNK in *Mettl3*-HKO hepatocytes. Mechanistically, METTL3 interacts with RNA polymerase II and active histone modifications such as H3K9ac, H3K27ac, and H3K36me3 to maintain the expression of proteasome-related genes.

Conclusions: Our study demonstrated that downregulation of METTL3 promotes APAP-induced liver injury by decreasing proteasome activity and thereby enhancing activity of the MKK4/JNK signalling pathway.

Impact and Implications: Acetaminophen (APAP) overdose is a key cause of acute liver failure in the Western world, but its molecular mechanisms are not fully understood. We demonstrated in this study that methyltransferase-like 3 (METTL3), a core m^{6}A RNA methyltransferase, is downregulated in APAP-induced liver injury, which exacerbates APAP-induced liver injury through enhancing the MKK4/JNK signalling pathway with involvement of the decreased proteasome activity.

Introduction

Acetaminophen (APAP) is one of the most commonly used drugs worldwide for the treatment of minor aches, pains, and fever. However, APAP overdose is also the predominant cause of acute liver failure in the Western world.[1–3] The hepatotoxicity of APAP overdose results from its reactive intermediate, *N*-acetyl-*p*-benzoquinone imine (NAPQI), produced by cytochrome P-450 2E1 (CYP2E1).[4,5] NAPQI depletes cellular glutathione (GSH) and then covalently binds to intracellular and mitochondrial proteins to form APAP adducts,[4] leading to mitochondrial dysfunction, oxidative stress, phosphorylation, and mitochondrial translocation of Jun NH2-terminal kinase (JNK)[6] and necrosis of hepatocytes.[7] JNK is critical for APAP-induced liver injury and cell death,[8,9] and inhibition of JNK by either a pharmacological inhibitor or gene knockdown protects against APAP-induced liver injury.[6] However, the activation of JNK during APAP-induced liver injury also requires the activation of its upstream kinases including apoptosis signal-regulating kinase 1 (ASK1),[10] glycogen synthase kinase-3 beta (GSK-3β),[11] mixed-lineage kinase 3 (MLK3),[12] receptor interacting protein kinase 1 (RIP1),[13] RIP3,[14] and mitogen-activated protein kinase kinase 4 (MKK4).[15] Deficiency of each of these kinases protects against APAP-induced liver injury.[10–15] In addition, several phosphatases including mitogen-activated protein kinase phosphatase 1 (MKP1) and protein tyrosine phosphatase 1B that counteract JNK activation have been reported to protect against APAP-induced liver injury.[16,17] Despite numerous studies in the past four decades,

Keywords: METTL3; Liver injury; m^{6}A; APAP; Inflammation.
Received 28 October 2022; received in revised form 6 April 2023; accepted 12 April 2023; available online 21 April 2023

† These authors contributed equally to this work.

* Corresponding author. Address: HIT Center for Life Sciences, School of Life Science and Technology, Harbin Institute of Technology, Harbin 150001, China. Tel.: +86-45186402029
E-mail address: chenzheng@hit.edu.cn (Z. Chen).

the detailed molecular mechanisms of APAP-induced liver injury and JNK activation remain to be elucidated.

N6-methyl-adenosine (m^6A) has been shown to be a reversible and dynamic mRNA modification, which is catalysed by methyltransferase-like 3 (METTL3), METTL14, and Wilms' tumor 1-associating protein (WTAP); recognised by YTH domain-containing protein 1-2 (YTHDC1-2) in the nucleus and YTH N6-methyladenosine RNA binding protein 1-3 (YTHDF1-3) in the cytosol; and removed by fat mass and obesity-associated (FTO) and AlkB homolog 5, RNA demethylase (ALKBH5).[18] METTL3 and m^6A-related proteins regulate many physiological and pathological processes such as circadian clock,[19] DNA damage response,[20] neurogenesis,[21] spermatogenesis,[22,23] stem cell differentiation,[24,25] cancer,[26] energy metabolism,[27,28] non-alcoholic steatohepatitis,[29,30] and diabetes.[31–35] However, whether METTL3 regulates APAP-induced liver injury is largely unknown.

Here we report that hepatic METTL3 is downregulated in APAP-induced liver injury, which promotes APAP-induced liver injury. Hepatocyte-specific deletion of *Mettl3* exacerbates APAP-induced liver injury, leading to increased mortality, which is likely as a result of decreased proteasome activity and increased protein stability of MKK4 and JNK, leading to enhanced JNK activation. Inhibition of JNK by SP600125 completely blocks APAP-induced liver injury in hepatocyte-specific *Mettl3* knockout (*Mettl3*-HKO) mice. Therefore, downregulation of *Mettl3* promotes APAP-induced liver injury through enhancing the MKK4/JNK signalling pathway with involvement of decreased proteasome activity.

Materials and methods

Animal experiments

Animal experiments were carried out in strict accordance with the Guide for the Care and Use of Laboratory Animals. Animal experiment protocols were approved by the Institutional Animal Care and Use Committee of Harbin Institute of Technology (HIT/IACUC). The approval number was IACUC-2018004. Mice were housed on a 12-h light/12-h dark cycle and fed a normal chow diet with free access to water. For APAP-induced liver injury, mice were fasted for 12 h and then injected with APAP (500, 600, or 750 mg/kg body weight). *Mettl3*$^{flox/flox}$ mice, in which exon 2 and exon 3 of the *Mettl3* gene were flanked by two loxp sites, were generated using the CRISPR-Cas9 technique as previously reported.[27] Blood samples were collected from orbital sinus. The serum alanine aminotransferase (ALT) and aspartate transferase (AST) activities were measured using an ALT and AST reagent set, respectively.[29,36] Proteasome activity in liver samples was measured using a Proteasome Activity Assay Kit (ab107921, Abcam) following the instructions.

Primary hepatocyte culture, adenoviral infection, and PI staining

Primary hepatocytes were isolated from C57BL/6 wild-type (WT), *Mettl3*$^{flox/flox}$, and *Mettl3*-HKO mice by liver perfusion with type II collagenase (Worthington Biochem, Lakewood, NJ, USA) and cultured at 37 °C in RPMI 1640 medium supplemented with 3% FBS. They were infected with Ad-βGal, Ad-FLAG-PSMB4, or Ad-FLAG-PSMB6 adenoviruses overnight. Primary hepatocytes from C57BL/6 WT mice were infected with Ad-βGal or Ad-FLAG-METTL3 adenoviruses overnight. Hepa1-6 cells were infected with Ad-Scramble, Ad-sh*Mettl3*-1, and Ad-sh*Mettl3*-2 adenovirus for 24 h and then infected with Ad-βGal and Ad-FLAG-METTL3 adenovirus overnight. The target sequences are scramble: UUCUCCGAACGUGUCACGUTT, sh*Mettl3*-1: GCUACCGUAUGGGACAUUA, and sh*Mettl3*-2: CGGCUAAGAAGUCAAGGAA. Cells were treated with or without APAP for 4 h. Propidium iodide (PI) staining was used to measure cell death. Cells were incubated with PI (3 mM) at 37 °C for 10 min.

Real-time quantitative PCR

Real-time quantitative PCR (RT-qPCR) was performed as shown previously.[37] Briefly, total RNA was extracted using the TriPure Isolation Reagent (Roche, Mannheim, Germany), and first-strand cDNA was synthesised using random primers and M-MLV Reverse Transcriptase (Promega, Madison, WI, USA). RT-qPCR was performed using a LightCycler 480 real-time PCR system (Roche). The expression of individual genes was normalised to the expression of 36B4. Primers for RT-qPCR are listed in Table S1.

Translation efficiency assay

In total, 200-mg liver samples were isolated from *Mettl3*$^{flox/flox}$ and *Mettl3*-HKO mice, quickly frozen, and pestled into powder in liquid nitrogen. Then, 600 μl polysome lysis buffer (20 mM Tris-HCl [pH 7.4], 150 mM NaCl, 5 mM $MgCl_2$, 1% Triton-100, 1 × protease inhibitor cocktail, 1 mM dithiothreitol (DTT), 100 μg/ml cycloheximide (CHX), 1 U/μl SUPERase In RNase Inhibitor [AM2694, Invitrogen]) was added. The sample was transferred into an Eppendorf (EP) Tube (0030108051, Eppendorf) and rotated for 10 min at 4 °C. The samples were further triturated using a 26-gauge needle 10 times and then centrifuged at 13,000 rpm for 10 min at 4 °C. The supernatant was transferred into new 1.5-ml EP Tubes, and the absorbance at 260 nm was measured using NanoDrop 2000 (Thermo Fisher Scientific, Wilmington, DE, USA). Moreover, 500 μl lysate (25–30 optical density (OD) at 260 nm) was carefully transferred into a sucrose gradient (15 to 55% sucrose gradient was made by The Gradient Master™ [Biocomp Instruments, Fredericton, New Brunswick, Canada]) and ultracentrifuged at 38,000 rpm for 3 h at 4 °C. Ribosome fractions were analysed and collected using Piston Gradient Fractionator™ (Biocomp Instruments, Fredericton, New Brunswick, Canada). Total RNA was isolated from each fraction, and reverse transcription-polymerase chain reaction (RT-PCR) was performed.

Chromatin immunoprecipitation assays

The livers were fixed by liver perfusion with 1% paraformaldehyde. The nuclei were isolated from livers and subjected to sonication (M220 Focused-ultrasonicator, Covaris, Massachusetts, USA) to break genomic DNA into 500- to 1,000-bp fragments using a chromatin shearing kit (520127 truChIP Chromatin Shearing Kit, Covaris). The samples were immunoprecipitated with anti-RNA polymerase II (Rpb1 CTD, 2629, Cell Signaling Technology). DNA was extracted and used for quantitative PCR analysis. Primers for quantitative PCR are listed in Table S1.

Immunoprecipitation and immunoblotting

Cells or tissues were homogenised in an L-RIPA lysis buffer (50 mM Tris, pH 7.5, 1% Nonidet P-40, 150 mM NaCl, 2 mM EGTA, 1 mM Na_3VO_4, 100 mM NaF, 10 mM $Na_4P_2O_7$, 1 mM phenylmethylsulfonyl fluoride). Proteins were separated by SDS-PAGE,

immunoblotted with the indicated antibodies, and visualised using enhanced chemiluminescence. Antibodies were as follows: FLAG (F1804, Sigma), JNK1 (A0288, Abclonal), JNK2 (A1251, Abclonal), JNK (9252, Cell Signaling Technology), p-JNK (9251, Cell Signaling Technology), p-MKK4 (9156, Cell Signaling Technology), MKK4 (9152, Cell Signaling Technology), METTL3 (96391, Cell Signaling Technology), PSMB4 (11029-1-AP, Proteintech), PSMB6 (11684-2-AP, Proteintech), CYP2E1 (19937-1-AP, Proteintech), Tubulin (sc5286, Santa Cruz), AIF (17984-1-AP, Proteintech), EndoG (22148-1-AP, Proteintech), and cytochrome c (Cytc) (ab13575, Abcam).

RNA sequencing

RNA sequencing (RNA-seq) was performed as described previously.[27,30,37,38] RNA-seq data that support the findings of this study have been deposited in Gene Expression Omnibus (GEO) under accession code GSE214371.

Liver ROS assays

Liver reactive oxygen species (ROS) assays have been described previously.[36] In brief, liver samples were homogenised in a L-RIPA buffer. Liver extracts were incubated with dichlorofluorescein diacetate fluorescent (5 μM) probes (D6883, Sigma-Aldrich) at 37 °C for 1 h. Fluorescence was measured and normalised to tissue weight.

Statistical analysis

Data are presented as means ± SEM. Differences between two groups were analysed using Student's *t* tests. Differences between three groups were analysed using one-factor ANOVA and the least significance difference *t* test. In all analyses, $p < 0.05$ was considered statistically significant ($^{*}p < 0.05$; $^{**}p < 0.01$).

Results

METTL3 is downregulated in APAP-induced liver injury mice

To determine whether METTL3 is associated with APAP-induced liver injury, C57BL/6 WT mice fasted overnight were treated with 500 mg/kg of APAP by i.p. injection, and the expression of METTL3 was measured by immunoblotting. METTL3 protein levels were markedly decreased in the livers of APAP-treated WT mice (Fig. 1A). METTL3 protein levels were also reduced in mouse primary hepatocytes by APAP in a dose-dependent manner (Fig. 1B). These data suggest that METTL3 is associated with APAP-induced liver injury, and downregulation of METTL3 may promote APAP-induced liver injury.

Hepatic deletion of *Mettl3* exacerbates APAP-induced liver injury

We then investigated the functional role of METTL3 in APAP-induced liver injury. We generated *Mettl3*-HKO mice by crossing *Mettl3*$^{flox/flox}$ with *Alb*-Cre mice as shown previously.[29] *Mettl3*$^{flox/flox}$ and *Mettl3*-HKO mice were administered an equal amount of APAP to induce liver injury. Hepatocyte-specific deletion of *Mettl3* exacerbated APAP-induced liver injury, as revealed by a marked increase in serum ALT/AST levels and hepatocyte loss in response to 500 mg/kg APAP treatment for 24 h (Fig. 1C and D). We noticed that *Mettl3*-HKO mice showed slight liver injury (higher basal serum ALT levels) before APAP treatment, which may promote APAP-induced liver injury. To determine whether 50% deletion of *Mettl3* in hepatocytes also exacerbates APAP-induced liver injury, heterozygous mice without liver injury and their control mice were injected with the same amount of APAP (600 mg/kg). As shown in Fig. 1E, 50% deletion of *Mettl3* in hepatocytes also exacerbates APAP-induced liver injury, as revealed by higher serum ALT levels after APAP treatment. Necrotic areas in the liver sections of *Mettl3*-HKO mice were significantly increased at 6 and 24 h after APAP injection (Fig. 1F and G). Furthermore, hepatic deletion of *Mettl3* also accelerated the acute liver injury induced by the high dose of APAP (750 mg/kg) and caused more mice to die (Fig. 1H). These results suggest a critical role for METTL3 in APAP-induced liver injury and hepatocyte death.

Hepatic deletion of *Mettl3* increases MKK4/JNK signalling pathway

Next, we asked whether deletion of *Mettl3* changed the APAP metabolism. The hepatotoxicity of APAP overdose results from its reactive intermediate (NAPQI), which is generated by CYP2E1.[4,5] As shown in Fig. 2A, we observed similar levels of CYP2E1 expression in the livers of *Mettl3*$^{flox/flox}$ and *Mettl3*-HKO mice treated with or without APAP. NAPQI depletes cellular GSH. We then measured the hepatic GSH levels before and after APAP treatment. As shown in Fig. 2B, the hepatic GSH levels were higher in the livers of *Mettl3*-HKO mice before APAP treatment, which is likely owing to changed expression of GSH metabolism-related genes (Fig. 2C). RNA-seq analysis showed that GSH formation-related genes were upregulated and GSH degradation-related genes were downregulated in *Mettl3*-HKO livers (Fig. 2C). However, APAP treatment depleted the cellular GSH to similar levels at 3 and 6 h after APAP treatment in *Mettl3*$^{flox/flox}$ and *Mettl3*-HKO mice (Fig. 2B). After APAP treatment for 24 h, *Mettl3*-HKO mice showed higher levels of cellular GSH (Fig. 2B), indicating that deletion of *Mettl3* increases cellular GSH levels, which is less likely to contribute to more severe APAP-induced liver injury in *Mettl3*-HKO mice.

Next, we asked whether mitochondrial dysfunction and oxidative stress contributed to more severe APAP-liver injury in *Mettl3*-HKO mice. Mitochondrial injury (release of mitochondrial proteins) and ROS levels were measured. As shown in Fig. 2D, the release of mitochondrial proteins such as AIF, EndoG, and Cytc did not change in APAP-treated *Mettl3*-HKO livers compared with that in APAP-treated *Mettl3*$^{flox/flox}$ livers. We also did not observe any difference in liver ROS levels between APAP-treated *Mettl3*-HKO and *Mettl3*$^{flox/flox}$ mice (Fig. 2E). These data indicate that mitochondrial dysfunction and oxidative stress are less likely to contribute to more severe APAP-induced liver injury in *Mettl3*-HKO mice.

The MKK4/JNK signalling pathway plays a key role in APAP-induced liver injury.[15] To determine whether METTL3 deficiency influences JNK signalling, we used immunoblotting to determine the activation of MKK4 and JNK at 6 h after APAP treatment in the livers from *Mettl3*$^{flox/flox}$ and *Mettl3*-HKO mice. As shown in Fig. 2F, p-MKK4 and p-JNK protein levels were significantly increased in the livers of *Mettl3*-HKO mice under both basal and APAP-treated conditions, and the MKK4 and JNK protein levels were also elevated, which indicates that activation of the MKK4 and JNK signalling pathway leads to enhanced APAP-induced liver injury in *Mettl3*-HKO mice. We also checked p-p38, p38, p-extracellular-signal-regulated kinase (ERK), and

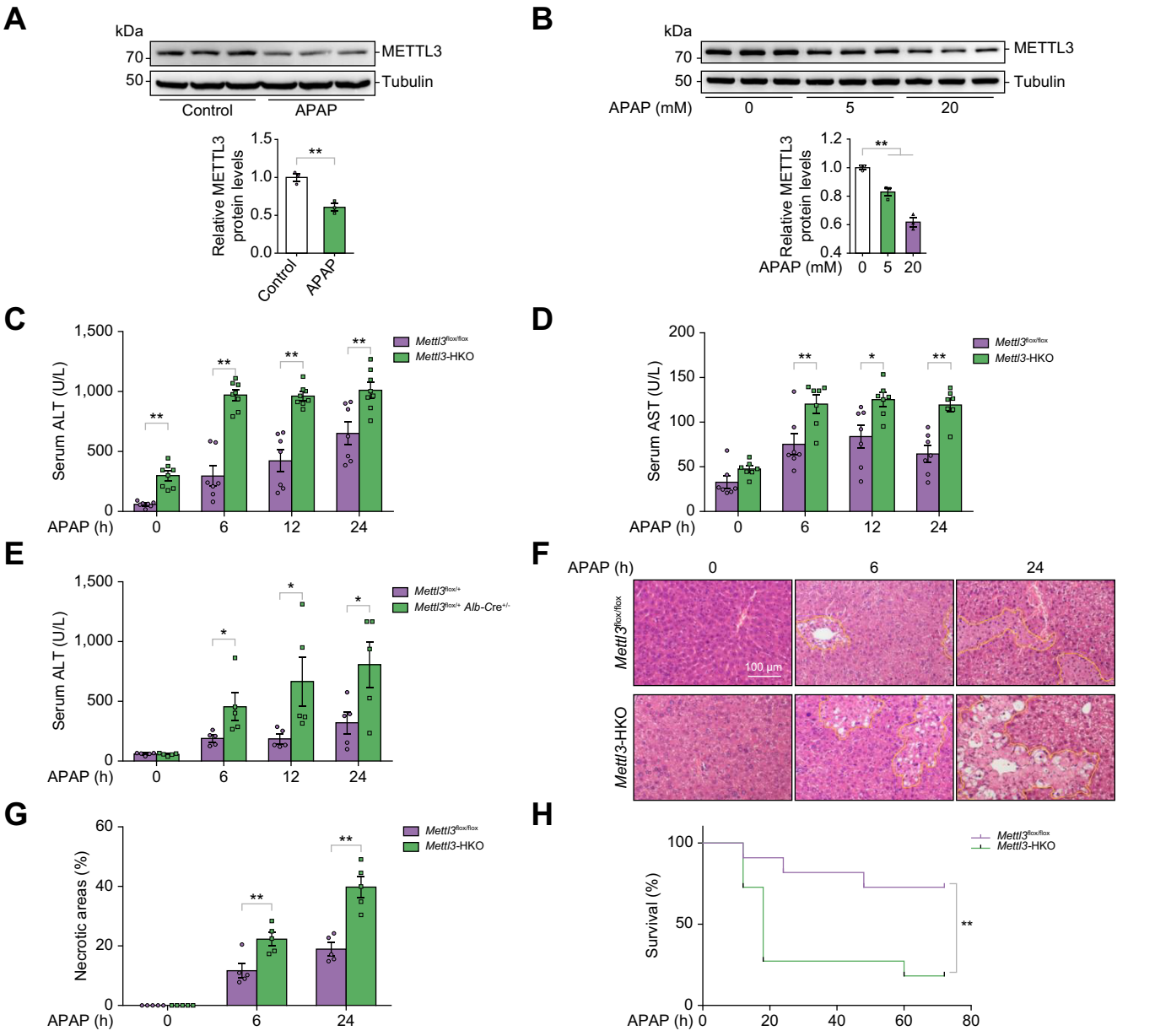

Fig. 1. Hepatic deletion of *Mettl3* exacerbates APAP-induced liver injury. (A) Eight-week-old C57BL/6 WT mice fasted overnight were treated with 500 mg/kg of APAP by i.p. injection, and METTL3 protein levels were measured by immunoblotting (n = 3 independent mice for each group, $p = 0.004$, Student's *t* tests). (B) Primary hepatocytes were isolated from C57BL/6 WT mice and then treated with APAP at different doses (0, 5, and 20 mM) for another 4 h. METTL3 protein levels were measured by immunoblotting (n = 3 independent cell samples for each group; 5 *vs.* 0 mM: $p = 0.0041$; 20 *vs.* 0 mM: $p = 0.0003$; Student's *t* tests). (C and D) *Mettl3*$^{flox/flox}$ and *Mettl3*-HKO mice were administered an equal amount of APAP (500 mg/kg). Mice were sacrificed at different time points (0, 6, 12, and 24 h) after APAP injection. Serum ALT and AST levels were measured (n = 7–8 mice for each group; ALT: 0 h, $p < 0.0001$; 6 h, $p < 0.0001$; 12 h, $p < 0.0001$; 24 h, $p = 0.0043$. AST: 0 h, $p = 0.0633$; 6 h, $p = 0.0093$; 12 h, $p = 0.0128$; 24 h, $p = 0.0003$; Student's *t* tests). (E) *Mettl3* heterozygous (*Mettl3*$^{flox/+}$ *Alb*-Cre$^{+/-}$) mice and their control mice administered an equal amount of APAP (600 mg/kg). Serum ALT levels were measured at different time points (0, 6, 12, and 24 h) after APAP injection (n = 5 mice for each group; 0 h, $p = 0.6191$; 6 h, $p = 0.0441$; 12 h, $p = 0.0452$; 24 h, $p = 0.0443$; Student's *t* tests). (F and G) Necrotic areas were measured by H&E staining and quantified by ImageJ in *Mettl3*$^{flox/flox}$ and *Mettl3*-HKO livers (n = 5 mice for each group; 6 h, $p = 0.0086$; 24 h, $p = 0.0006$; Student's *t* tests). (H) *Mettl3*$^{flox/flox}$ and *Mettl3*-HKO mice were administered an equal amount of APAP (750 mg/kg). Mouse survival curve was measured (n = 11 mice for each group, $p = 0.0089$; Student's *t* tests). Differences between two groups were analysed using Student's *t* tests. $^{*}p < 0.05$. $^{**}p < 0.01$. Data represent the mean ± SEM. ALT, alanine aminotransferase; APAP, acetaminophen; AST, aspartate transferase; *Mettl3*-HKO, hepatocyte-specific *Mettl3* knockout; METTL3, methyltransferase-like 3; WT, wild-type.

ERK levels. As shown in Fig. S1, p-p38 and p38 levels were similar, whereas both p-ERK and ERK levels were significantly increased in *Mettl3*-HKO livers, indicating that METTL3 regulates both JNK and ERK signalling pathways.

JNK inhibitor blocks APAP-induced liver injury in *Mettl3*-HKO mice

JNK plays an essential role in APAP-induced liver injury, and higher activation of the JNK signalling pathway was also observed in

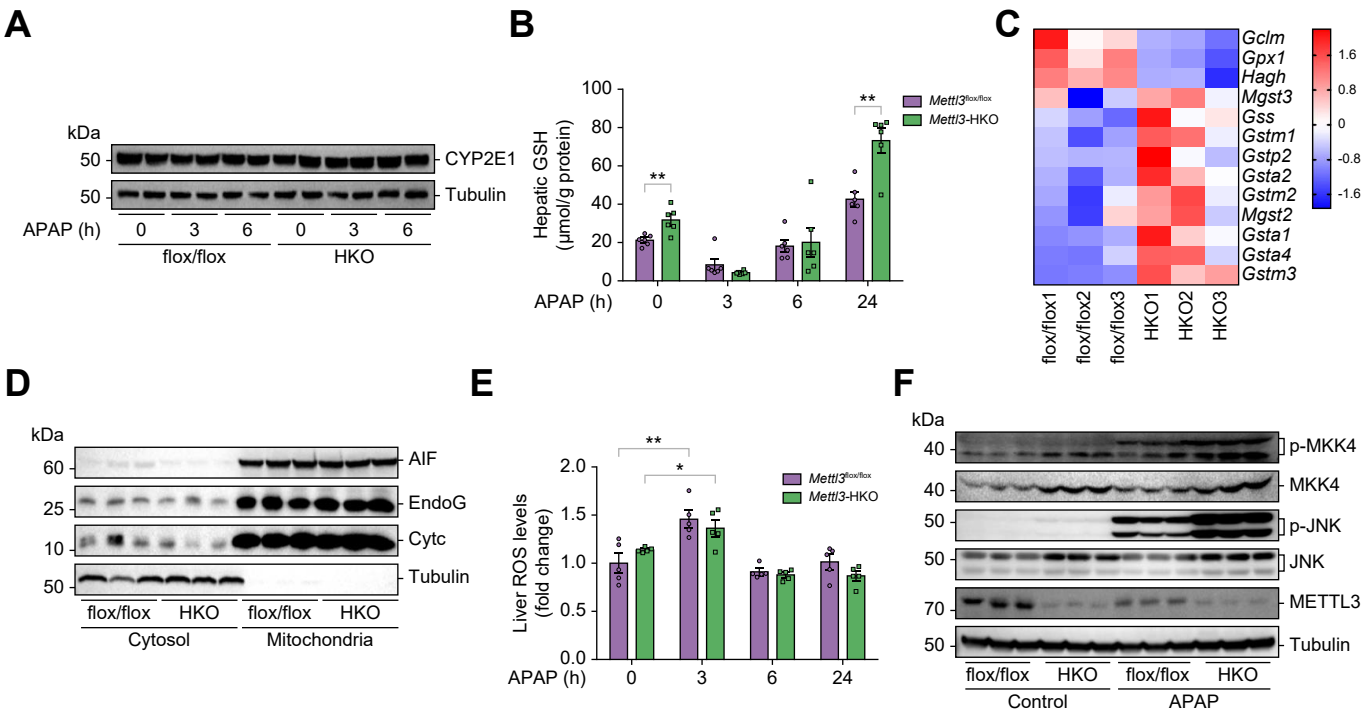

Fig. 2. Hepatic deletion of *Mettl3* activates the MKK4/JNK signalling pathway. *Mettl3*$^{flox/flox}$ and *Mettl3*-HKO mice at 8 weeks old were administered an equal amount of APAP (500 mg/kg). Mice were sacrificed at different time points (0, 3, 6, and 24 h) after APAP injection. (A) CYP2E1 protein levels were measured in the livers of *Mettl3*$^{flox/flox}$ and *Mettl3*-HKO mice injected with APAP for different time points (0, 3, and 6 h). (B) Hepatic GSH levels were measured by ELISA in the livers of *Mettl3*$^{flox/flox}$ and *Mettl3*-HKO mice injected with APAP for different time points (0, 3, 6, and 24 h) (n = 6 mice for each group; 0 h, $p = 0.0042$; 3 h, $p = 0.1769$; 6 h, $p = 0.7993$; 24 h, $p = 0.0013$; Student's *t* tests). (C) Heatmap of GSH metabolism-related genes is shown. (D) Cytosol and mitochondria were isolated by centrifuge from livers of *Mettl3*$^{flox/flox}$ and *Mettl3*-HKO mice injected with APAP. The release of mitochondrial proteins such as AIF, EndoG, and Cytc was measured by immunoblotting (n = 3 mice for each group). (E) Liver ROS levels were measured (n = 5 mice for each group; 0 h, $p = 0.1904$; 3 h, $p = 0.4473$; 6 h, $p = 0.4388$; 24 h, $p = 0.1263$; Student's *t* tests). (F) p-MKK4, MKK4, p-JNK, JNK, METTL3, and Tubulin protein levels in the livers of *Mettl3*$^{flox/flox}$ and *Mettl3*-HKO mice injected with APAP for 6 h were measured by immunoblotting. Immunoblotting experiments were repeated three times independently with similar results. Differences between two groups were analysed by Student's *t* tests. $^{*}p$ <0.05. $^{**}p$ <0.01. Data represent the mean ± SEM. APAP, acetaminophen; CYP2E1, cytochrome P-450 2E1; Cytc, cytochrome c; GSH, glutathione; *Mettl3*-HKO, hepatocyte-specific *Mettl3* knockout; METTL3, methyltransferase-like 3; ROS, reactive oxygen species.

Mettl3-HKO mice. Next, we asked whether inhibition of JNK could block APAP-induced liver injury in *Mettl3*-HKO mice. *Mettl3*$^{flox/flox}$ and *Mettl3*-HKO mice were pretreated with a JNK inhibitor (SP600125) or vehicle and then treated with APAP (500 mg/kg) to induce liver injury. As expected, *Mettl3*-HKO mice showed more severe liver injury, as revealed by a marked increase in serum ALT/AST levels and more necrotic areas in response to APAP treatment for 24 h (Fig. 3A–C). However, SP600125 completely inhibited APAP-induced liver injury in *Mettl3*-HKO mice (Fig. 3A–C), which was most likely owing to the complete blockage of APAP-induced phosphorylation of JNK (Fig. 3D). These data indicate that down-regulation of METTL3 aggravates APAP-induced liver injury mainly through activation of JNK.

Hepatic deficiency of *Mettl3* increases protein stability of MKK4/JNK

Next, we tried to answer how hepatic deficiency of *Mettl3* causes the activation of MKK4/JNK. The protein levels of MKK4 and JNK1/2 were increased in the livers and isolated hepatocytes from *Mettl3*-HKO mice (Fig. 4A and B), whereas their mRNA levels were not increased (Fig. 4C), which indicates that hepatic deficiency of *Mettl3* increases translational efficiency or protein stability. We then measured the translational efficiency in *Mettl3*$^{flox/flox}$ and *Mettl3*-HKO mice by performing sucrose gradient centrifugation to resolve polysome fractions of *Mettl3*-HKO and *Mettl3*$^{flox/flox}$ livers and using RT-PCR to measure the distribution of endogenous *Mkk4*, *Jnk1*, and *Jnk2* mRNA levels in different ribosome fractions. As shown in Fig. 4D, the relative distribution of mRNAs of *Mkk4* and *Jnk1/2* in polysome fractions was not changed in *Mettl3*-HKO mice, indicating that hepatic deletion of *Mettl3* does not affect the translational efficiency of *Mkk4* and *Jnk1/2* mRNA. We also measured the protein stability of MKK4 and JNK1/2. As shown in Fig. 4E, the protein stability was dramatically increased in isolated hepatocytes from *Mettl3*-HKO mice, whereas the mRNA levels of *Mkk4* and *Jnk1/2* were unchanged or decreased before or after cycloheximide treatment (Fig. S2). These data demonstrate that hepatic deficiency of *Mettl3* increases protein stability of MKK4 and JNK1/2.

Hepatic deficiency of *Mettl3* decreases proteasome activity, which contributes to the increased protein stability of MKK4 and JNK

To determine how hepatic deficiency of *Mettl3* increases protein stability of MKK4 and JNK1/2, we performed RNA-seq analysis. Consistent with previous RNA-seq data,[29] Kyoto Encyclopedia of

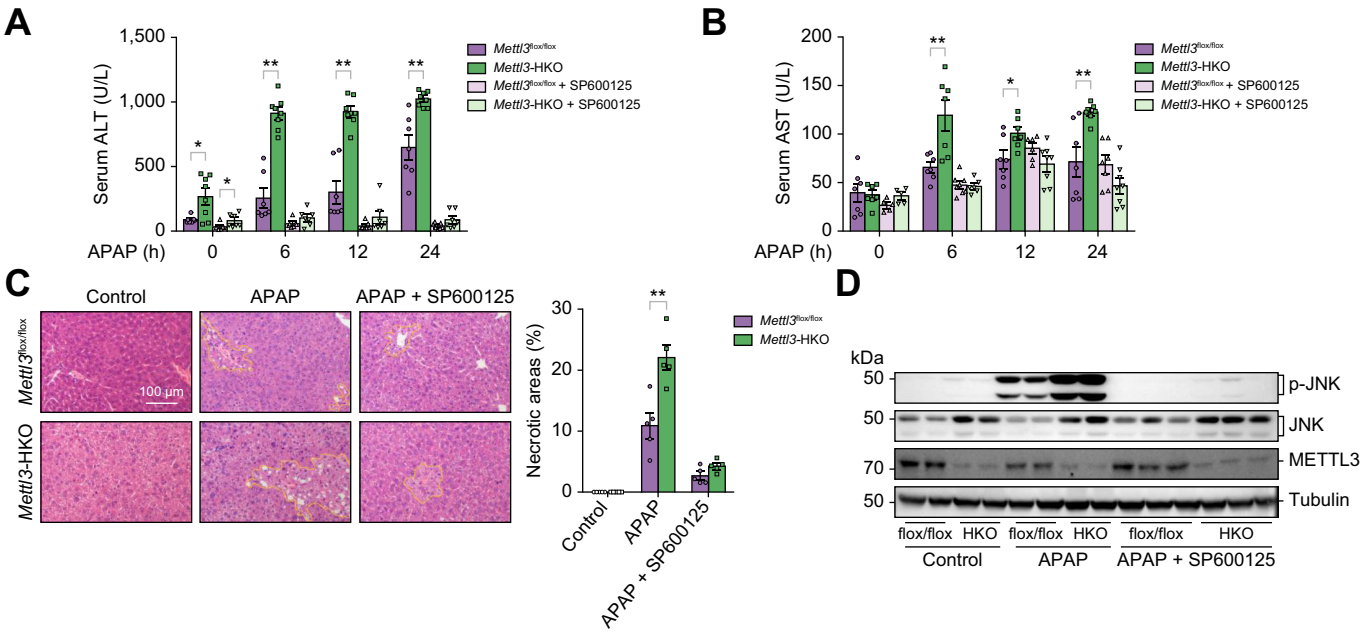

Fig. 3. JNK inhibitor blocks APAP-induced liver injury in *Mettl3*-HKO mice. *Mettl3*$^{flox/flox}$ and *Mettl3*-HKO mice were pretreated with or without a JNK inhibitor (SP600125, 20 mg/kg) for 2 h and then treated with APAP (500 mg/kg) to induce liver injury. (A and B) Serum was collected at different time points (0, 6, 12, and 24 h) after APAP injection. Serum ALT and AST levels were measured (n = 5–8 mice for each group; for serum ALT, *Mettl3*-HKO *vs.* *Mettl3*$^{flox/flox}$: 0 h, $p = 0.0139$; 6 h, $p < 0.0001$; 12 h, $p < 0.0001$; 24 h, $p = 0.0009$; *Mettl3*-HKO + SP600125 *vs.* *Mettl3*$^{flox/flox}$ + SP600125: 0 h, $p = 0.0468$; 6h, $p = 0.1155$; 12 h, $p = 0.1617$; 24 h, $p = 0.0904$; for serum AST, *Mettl3*-HKO *vs.* *Mettl3*$^{flox/flox}$: 0 h, $p = 0.8265$; 6 h, $p = 0.0051$; 12 h, $p = 0.0211$; 24 h, $p = 0.0051$; *Mettl3*-HKO + SP600125 *vs.* *Mettl3*$^{flox/flox}$ + SP600125: 0 h, $p = 0.0568$; 6 h, $p = 0.7937$; 12 h, $p = 0.1017$; 24 h, $p = 0.0801$; Student's *t* tests). (C) Necrotic areas in the livers of *Mettl3*$^{flox/flox}$ and *Mettl3*-HKO mice injected with APAP for 6 h were measured by H&E staining and quantified by ImageJ (n = 5 mice for each group; APAP, $p = 0.0038$; APAP + SP600125, $p = 0.0626$; Student's *t* tests). (D) p-JNK, JNK, METTL3, and Tubulin protein levels in the livers of *Mettl3*$^{flox/flox}$ and *Mettl3*-HKO mice injected with APAP for 6 h were measured by immunoblotting. Immunoblotting experiments were repeated three times independently with similar results. Differences between two groups were analysed using Student's *t* tests. $^{*}p < 0.05$. $^{**}p < 0.01$. Data represent the mean ± SEM. ALT, alanine aminotransferase; APAP, acetaminophen; AST, aspartate transferase; *Mettl3*-HKO, hepatocyte-specific *Mettl3* knockout; METTL3, methyltransferase-like 3.

Genes and Genomes (KEGG) pathway analysis showed that the downregulated genes were associated with steroid hormone biosynthesis, peroxisome, chemical carcinogenesis, proteasome, and oxidative phosphorylation (Fig. 5A), whereas the upregulated genes were associated with cell adhesion molecules, *Staphylococcus aureus* infection, viral protein interaction with cytokine and cytokine receptor, and chemokine signalling pathway (Fig. S3). We noticed that 23 proteasome-associated genes were downregulated (Fig. 5A and B), which was further confirmed by RT-qPCR (Fig. S4). Proteasome activity was decreased (Fig. 5C), and proteasome 20S subunit beta 4 (PSMB4)/PSMB6 (key components of proteasome) protein levels were significantly reduced in the livers of *Mettl3*-HKO mice (Fig. 5D). However, inhibition of proteasome by MG132 did not change the GSH levels in primary hepatocytes (Fig. S5), indicating that decreased proteasome activity is less likely to contribute to the increased GSH levels in *Mettl3*-HKO livers. Interestingly, APAP-induced liver injury also showed decreased proteasome activity and protein levels of PSMB4 and PSMB6 (Fig. S6A and B). These data indicate that decreased proteasome activity may lead to increased stability of MKK4 and JNK1/2.

Next, we asked whether restoration of proteasome activity by overexpression of PSMB4 and PSMB6 could reverse the higher protein levels of MKK4 and JNK. Adenovirus-mediated overexpression of PSMB4 or PSMB6 decreased the higher protein levels of MKK4 and JNK in primary hepatocytes isolated from *Mettl3*-HKO mice (Fig. 5E and F). These data indicate that hepatic deficiency of *Mettl3* decreases proteasome activity, which contributes to the increased protein stability of MKK4 and JNK.

METTL3 decreases MKK4 and JNK protein levels by upregulating PSMB4 and PSMB6, which protects hepatocytes from APAP-induced hepatocyte death

To determine whether METTL3 negatively regulates MKK4/JNK protein levels by upregulating PSMB4 and PSMB6, which protects hepatocytes from APAP-induced hepatocyte death, we performed cell culture experiments. As shown in Fig. 6A and B, overexpression of METTL3 in both primary hepatocytes and Hepa1-6 cells decreased MKK4 and JNK protein levels but increased PSMB4 and PSMB6 protein levels. Overexpression of METTL3 in Hepa1-6 also protected hepatocytes from APAP-induced cell death (Fig. 6C). Conversely, knockdown of *Mettl3* by infecting with Ad-sh*Mettl3*-1 and Ad-sh*Mettl3*-2, respectively, increased MKK4 and JNK protein levels but decreased PSMB4 and PSMB6 protein levels (Fig. 6D). METTL3 overexpression could reverse their expression in *Mettl3* knockdown Hepa1-6 cells (Fig. 6D). Knockdown of *Mettl3* promoted APAP-induced

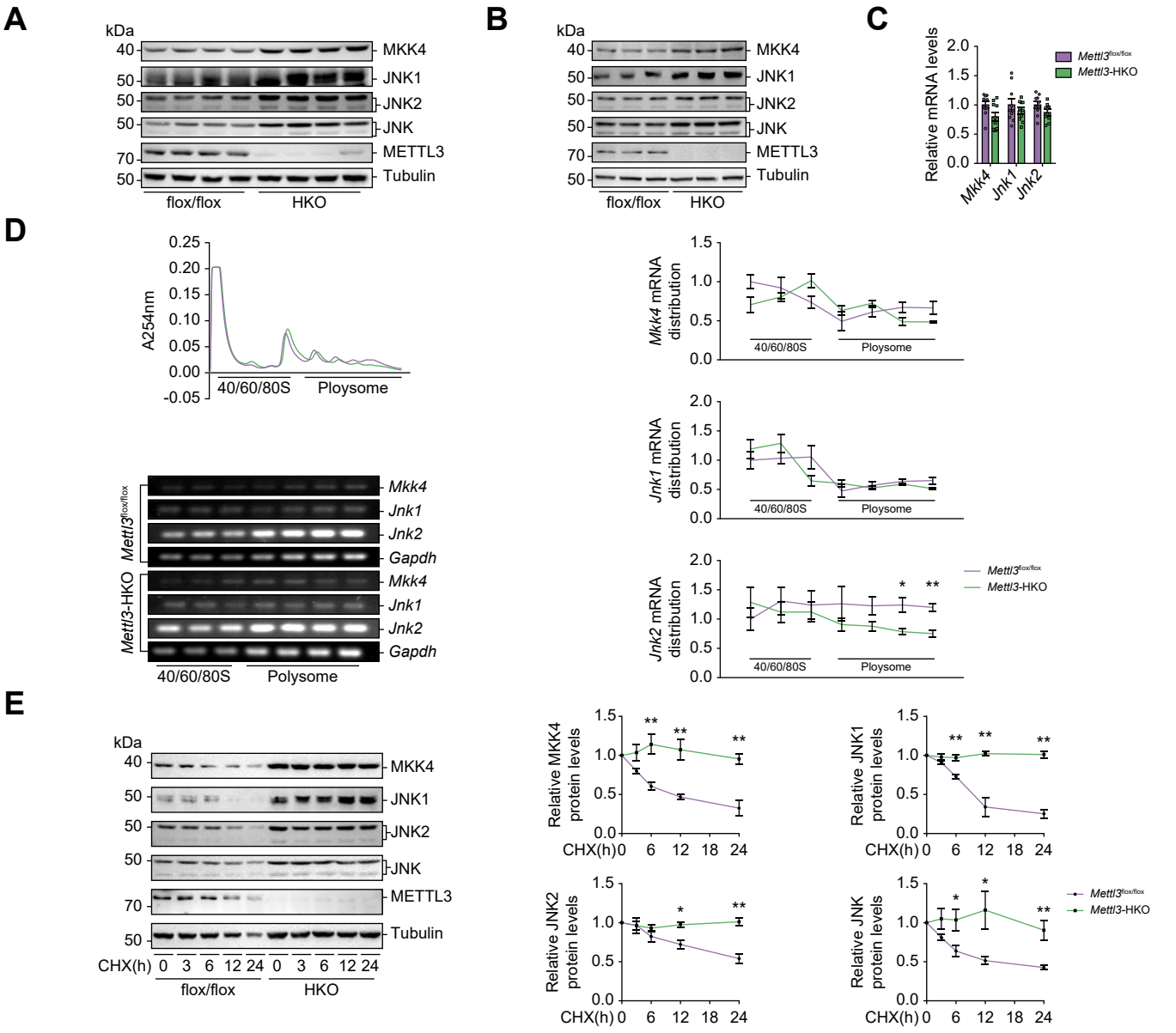

Fig. 4. Hepatic deficiency of *Mettl3* increases protein stability of MKK4 and JNK. (A and B) The protein levels of MKK4 and JNK1/2 were measured by immunoblotting in the livers (n = 4 mice for each group) and isolated hepatocytes (n = 3 independent cell samples for each group) from *Mettl3*-HKO and *Mettl3*$^{flox/flox}$ mice. (C) The mRNA levels of *Mkk4* and *Jnk1/2* in the livers of *Mettl3*-HKO and *Mettl3*$^{flox/flox}$ mice were measured by RT-qPCR (n = 10 mice for each group; *Mkk4*, $p = 0.093$; *Jnk1*, $p = 0.1073$; *Jnk2*, $p = 0.2092$; Student's *t* tests). (D) The fractions of 40s, 60s, 80s, and polysomes in the livers of *Mettl3*-HKO and *Mettl3*$^{flox/flox}$ mice were identified by sucrose gradient centrifugation. The relative distribution of *Mkk4* and *Jnk1/2* mRNAs in these fractions was measured by semi-quantitative RT-PCR (n = 3 mice for each group; *Mkk4*: 40s, $p = 0.0827$; 60s, $p = 0.4564$; 80s, $p = 0.0663$; polysome: $p = 0.3527$; $p = 0.1451$; $p = 0.0635$; $p = 0.0786$; *Jnk1*: 40s, $p = 0.4060$; 60s, $p = 0.2259$; 80s, $p = 0.1228$; polysome: $p = 0.3317$; $p = 0.5025$; $p = 0.3025$; $p = 0.0604$; *Jnk2*: 40s, $p = 0.4041$; 60s, $p = 0.5367$; 80s, $p = 0.6924$; polysome: $p = 0.3068$; $p = 0.0932$; $p = 0.0235$; $p = 0.0046$; Student's *t* tests). (E) Primary hepatocytes were isolated from *Mettl3*-HKO and *Mettl3*$^{flox/flox}$ mice, and then treated with CHX (3 μg/ml) for different time points (0, 3, 6, 12, and 24 h). MKK4, JNK1, JNK2, JNK, METTL3, and Tubulin protein levels were measured by immunoblotting and quantified by ImageJ (n = 3–4 mice for each group; MKK4: 3 h, $p = 0.0648$; 6 h, $p = 0.0059$; 12 h, $p = 0.0031$; 24 h, $p = 0.0014$; JNK1: 3 h, $p = 0.1547$; 6 h, $p = 0.0034$; 12 h, $p = 0.0042$; 24 h, $p = 0.0003$; JNK2: 3 h, $p = 0.9887$; 6 h, $p = 0.2219$; 12 h, $p = 0.0118$; 24 h, $p = 0.0026$; JNK: 3 h, $p = 0.1232$; 6 h, $p = 0.0398$; 12 h, $p = 0.0349$; 24 h, $p = 0.0086$; Student's *t* tests). This experiment was repeated four times independently with similar results. Differences between two groups were analysed using Student's *t* tests. $^{*}p$ <0.05. $^{**}p$ <0.01. Data represent the mean ± SEM. CHX, cycloheximide; *Mettl3*-HKO, hepatocyte-specific *Mettl3* knockout; METTL3, methyltransferase-like 3; RT-PCR, reverse transcription-polymerase chain reaction; RT-qPCR, real-time quantitative PCR.

cell death in Hepa1-6 cells, whereas overexpression of METTL3 reversed APAP-induced cell death in *Mettl3* knockdown Hepa1-6 cells (Fig. 6E). These data indicate that METTL3 negatively regulates MKK4/JNK protein levels by upregulating PSMB4 and PSMB6, which protects hepatocytes from APAP-induced hepatocyte death.

METTL3 interacts with RNA polymerase II and active histone modifications such as H3K9ac, H3K27ac, and H3K36me3, which is required for maintaining the expression of proteasome-related genes

METTL3 is a key m^{6}A RNA methyltransferase. We then analysed our previous methylated RNA immunoprecipitation-sequencing

A

KEGG analysis of downregulated genes in *Mettl3*-HKO mice

KEGG ID	Description	Count	*p* value
mmu00140	Steroid hormone biosynthesis	34	1.89E-12
mmu05016	Huntington disease	75	5.35E-12
mmu05012	Parkinson disease	66	1.09E-11
mmu04146	Peroxisome	31	1.21E-11
mmu05204	Chemical carcinogenesis	34	1.75E-11
mmu00830	Retinol metabolism	31	2.54E-10
mmu05010	Alzheimer disease	78	3.95E-10
mmu03050	Proteasome	23	4.57E-10
mmu00190	Oxidative phosphorylation	42	7.65E-10

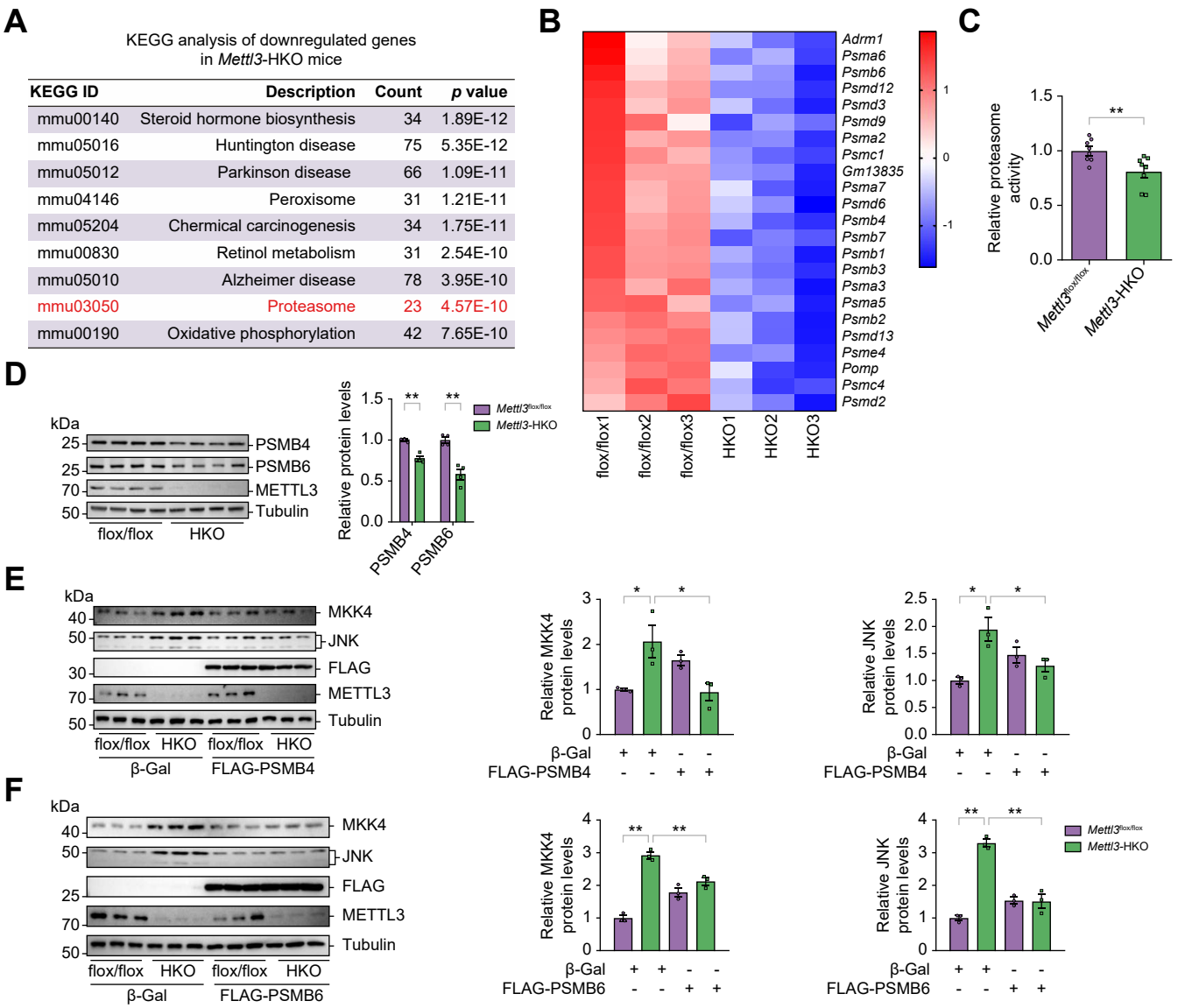

Fig. 5. Hepatic deficiency of *Mettl3* decreases proteasome activity, which contributes to the increased protein stability of MKK4 and JNK. (A and B) RNA-seq analysis was performed in the livers of *Mettl3*$^{flox/flox}$ and *Mettl3*-HKO mice at 8 weeks old (n = 3 for each group). KEGG pathway analysis of the downregulated genes in *Mettl3*-HKO mice (A). A heatmap of downregulated proteasome-related genes is shown (B). (C and D) Proteasome activity (n = 8 mice for each group, p = 0084; Student's t tests) and PSMB4/6 protein levels (n = 4 mice for each group; PSMB4, p = 0.0002; PSMB6, p = 0.0009; Student's t tests) were measured in the livers of *Mettl3*$^{flox/flox}$ and *Mettl3*-HKO mice. (E and F) Primary hepatocytes were isolated from *Mettl3*-HKO and *Mettl3*$^{flox/flox}$ mice and then infected with Ad-βGal, Ad-FLAG-PSMB4, and Ad-FLAG-PSMB6 adenovirus. MKK4, JNK, FLAG, METTL3, and Tubulin protein levels were measured by immunoblotting and quantified by ImageJ (n = 3 independent samples for each group; for MKK4 in (E), *Mettl3*-HKO + βGal *vs.* *Mettl3*$^{flox/flox}$+βGal, p = 0.0381; *Mettl3*-HKO + βGal *vs.* *Mettl3*-HKO + FLAG-PSMB4, p = 0.0466; for JNK in (E), *Mettl3*-HKO + βGal *vs.* *Mettl3*$^{flox/flox}$ + βGal, p = 0.0121; *Mettl3*-HKO + βGal *vs.* *Mettl3*-HKO+ FLAG-PSMB4, p = 0.0479; for MKK4 in (F), *Mettl3*-HKO + βGal *vs.* *Mettl3*$^{flox/flox}$ + βGal, p <0.0001; *Mettl3*-HKO + βGal *vs.* *Mettl3*-HKO+ FLAG-PSMB6, p = 0.0051; for JNK in (F), *Mettl3*-HKO + βGal *vs.* *Mettl3*$^{flox/flox}$ + βGal, p<0.0001; *Mettl3*-HKO + βGal *vs.* *Mettl3*-HKO + FLAG-PSMB6, p = 0.0014; Student's t tests). These experiments were repeated three times independently with similar results. Differences between two groups were analysed using Student's t tests. $^{*}p$ <0.05. $^{**}p$ <0.01. Data represent the mean ± SEM. KEGG, Kyoto Encyclopedia of Genes and Genomes; *Mettl3*-HKO, hepatocyte-specific *Mettl3* knockout; METTL3, methyltransferase-like 3; RNA-seq, RNA sequencing.

(MeRIP-seq) data collected from livers of *Mettl3*$^{flox/flox}$ and *Mettl3*-HKO mice and found that the m^{6}A peaks of some transcripts encoding proteasome components including *Psmb4* and *Psmb6* transcripts were decreased. Next, we tested whether mRNA stability and translational efficiency of *Psmb4* and *Psmb6* were decreased in *Mettl3*-HKO mice. As shown in Fig. 7A and B, neither mRNA stability nor translational efficiency of *Psmb4* and *Psmb6* was changed in *Mettl3*-HKO mice. METTL3 has also been shown to regulate gene transcription.[29] We analysed our previous assay for transposase-accessible chromatin with sequencing (ATAC-seq) data collected from livers of *Mettl3*$^{flox/flox}$ and *Mettl3*-HKO mice and found that 14 proteasome-related genes showed downregulated peaks. Combined analysis of the ATAC-seq and RNA-seq data showed that five proteasome-related genes, namely, *Psma6*, *Psmb3*, *Psmb4*, *Psmb6*, and *Gm13835*, were downregulated in *Mettl3*-HKO mice (Fig. 7C). These data indicate

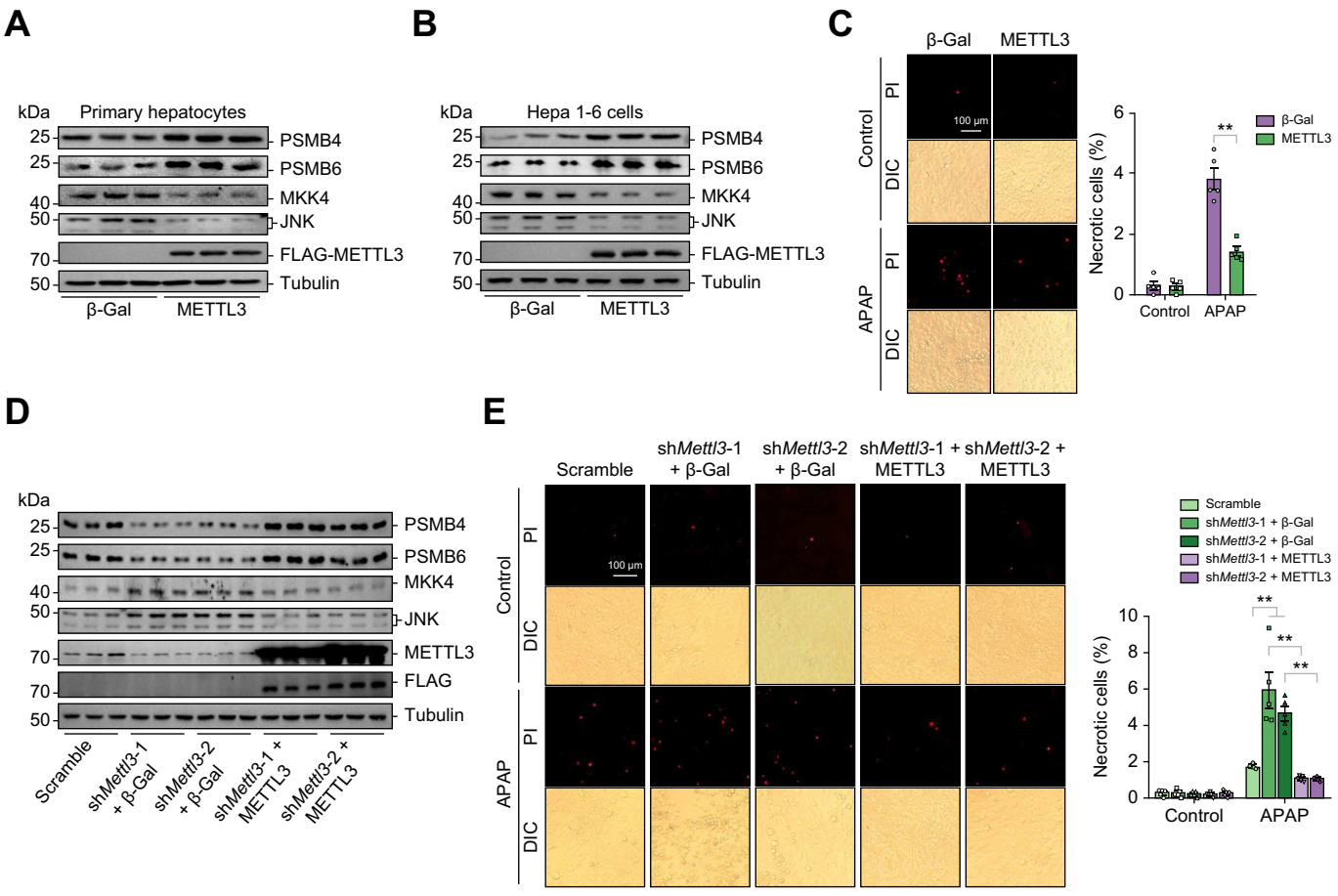

Fig. 6. METTL3 decreases MKK4 and JNK protein levels by upregulating PSMB4 and PSMB6, which protects hepatocytes from APAP-induced hepatocyte death. (A) Primary hepatocytes were isolated from C57BL/6 WT mice and then infected with Ad-βGal and Ad-FLAG-METTL3 adenovirus overnight. MKK4, JNK, PSMB4, PSMB6, FLAG, and Tubulin protein levels were measured by immunoblotting (n = 3 for each group). (B) Hepa1-6 cells were infected with Ad-βGal and Ad-FLAG-METTL3 adenovirus overnight. MKK4, JNK, PSMB4, PSMB6, FLAG, and Tubulin protein levels were measured by immunoblotting (n = 3 for each group). (C) Hepa1-6 cells were infected with Ad-βGal and Ad-FLAG-METTL3 adenovirus overnight and then treated with or without APAP for 4 h. PI staining was used to measure cell death (n = 5 for each group; Control, $p = 0.8507$; APAP, $p = 0.0001$; Student's *t* tests). (D and E) Hepa1-6 cells were infected with Ad-Scramble, Ad-sh*Mettl3*-1, and Ad-sh*Mettl3*-2 adenovirus for 24 h and then infected with Ad-βGal and Ad-FLAG-METTL3 adenovirus overnight. Some of the cells were used for measuring MKK4, JNK, PSMB4, PSMB6, FLAG, and Tubulin protein levels by immunoblotting (D) (n = 3 for each group). Some of the cells were treated with or without APAP for 4 h. PI staining was used to measure cell death (E) (n = 5 for each group; Control: βGal + sh*Mettl3*-1 *vs*. Scramble, $p = 0.8283$; βGal + sh*Mettl3*-2 *vs*. Scramble, $p = 0.5396$; sh*Mettl3*-1 + FLAG-METTL3 *vs*. Scramble, $p = 0.3924$; sh*Mettl3*-2 + FLAG-METTL3 *vs*. Scramble, $p = 0.8175$; APAP: βGal + sh*Mettl3*-1 *vs*. Scramble, $p = 0.0003$; βGal + sh*Mettl3*-2 *vs*. Scramble, $p = 0.0043$; βGal + sh*Mettl3*-1 *vs*. sh*Mettl3*-1 + FLAG-METTL3, $p = 0.0009$; βGal + sh*Mettl3*-2 *vs*. sh*Mettl3*-2 + FLAG-METTL3, $p < 0.0001$; ANOVA, LSD *t* test). $^{*}p < 0.05$. $^{**}p < 0.01$. Data represent the mean ± SEM. APAP, acetaminophen; DIC, differential interference contrast; *Mettl3*-HKO, hepatocyte-specific *Mettl3* knockout; METTL3, methyltransferase-like 3; PI, propidium iodide; WT, wild-type.

that hepatic deletion of *Mettl3* reduces transcription of these genes.

It has been shown that METTL14/METTL3 regulates gene expression by binding to RNA polymerase II and H3K36me3.[39] In primary hepatocytes, we observed that METTL3 also interacted with RNA polymerase II (Rpb1 CTD) and active histone modifications such as H3K9ac, H3K27ac, and H3K36me3 (Fig. 7D). Chromatin immunoprecipitation assay showed that the binding of RNA polymerase II (Rpb1 CTD) with genes of *Psma6*, *Psmb3*, *Psmb4*, and *Psmb6* was decreased in the livers of *Mettl3*-HKO mice, whereas the binding of RNA polymerase II (Rpb1 CTD) with genes of *Actb* did not change (Fig. 7E). These data indicate that METTL3 is required for maintaining expression of proteasome components by binding to RNA polymerase II and active histone modifications such as H3K9ac, H3K27ac, and H3K36me3.

Discussion

APAP overdose is a major cause of acute liver failure in Western countries. Early GSH depletion and JNK activation contribute to APAP-induced liver failure.[7,8] Whether this processing is regulated by RNA modification-related enzymes is not known. In this study, we demonstrated for the first time that APAP overdose causes downregulation of METTL3 (a key enzyme for m^6A mRNA modification), which in turn exacerbates APAP-induced hepatotoxicity by enhancing the JNK signalling pathway. Hepatic deficiency of *Mettl3* accelerates APAP-induced hepatotoxicity, leading to increased mortality. Mechanistically, *Mettl3* deficiency decreases gene transcription and m^6A mRNA modification of several components of proteasome, leading to decreased activity of proteasome and then increased protein stability of MKK4/JNK.

In APAP-induced liver injury, the metabolism of APAP to the reactive metabolite NAPQI by CYP2E1 represents the initial step

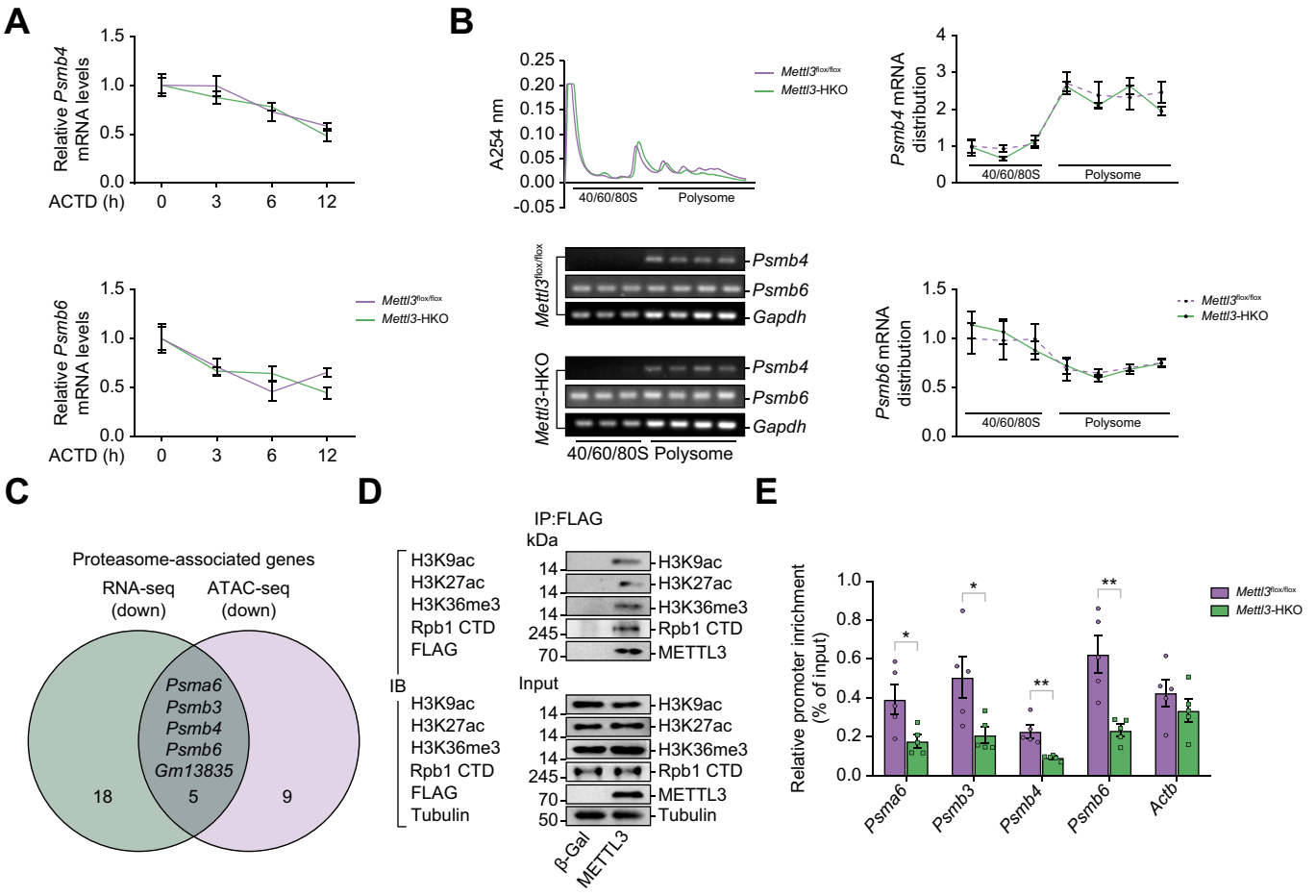

Fig. 7. METTL3 interacts with RNA polymerase II (Rpb1 CTD) and active histone modifications such as H3K9ac, H3K27ac, and H3K36me3, which is required for maintaining the expression of proteasome-related genes. (A) Primary hepatocytes were isolated from *Mettl3*-HKO and *Mettl3*$^{flox/flox}$ mice and then treated with actinomycin D (ACTD) (10 μg/mL) for different time points (0, 3, 6, and 12 h). *Psmb4* and *Psmb6* mRNA levels were measured by RT-qPCR (n = 6 independent cell samples for each group; *Psmb4*: 3 h, $p = 0.3232$; 6 h, $p = 0.6135$; 12 h, $p = 0.1166$; *Psmb6*: 3 h, $p = 0.6464$; 6 h, $p = 0.1429$; 12 h, $p = 0.012$; Student's *t* tests). (B) The fractions of 40s, 60s, 80s, and polysomes in the livers of *Mettl3*-HKO and *Mettl3*$^{flox/flox}$ mice were identified by sucrose gradient centrifugation. The relative distribution of mRNAs of *Psmb4* and *Psmb6* in these fractions was measured by semiquantitative RT-PCR (n = 3 mice for each group; *Psmb4*: 40s, $p = 0.9242$; 60s, $p = 0.0454$; 80s, $p = 0.6224$; polysome: $p = 0.7855$; $p = 0.4753$; $p = 0.4564$; $p = 0.1707$; *Psmb6*: 40s, $p = 0.5247$; 60s, $p = 0.7162$; 80s, $p = 0.5408$; polysome: $p = 0.8025$; $p = 0.2729$; $p = 0.7528$; $p = 0.9169$; Student's *t* tests). (C) Combined analysis of the ATAC-seq and RNA-seq data showed that five proteasome-related genes, namely, *Psma6*, *Psmb3*, *Psmb4*, *Psmb6* and *Gm13835*, were downregulated in *Mettl3*-HKO mice. (D) Primary hepatocytes were isolated from C57BL/6 WT mice and then infected with βGal and FLAG-METTL3 adenovirus. Total cell lysates were incubated with DNase1 (200 U/ml) at 37 °C for 30 min. These cell lysates were immunoprecipitated with FLAG beads and then immunoblotted with anti-H3K9ac, anti-H3K27ac, anti-H3K36me3, anti-Rpb1 CTD, and anti-FLAG antibodies. This experiment was repeated twice independently with similar results. (E) RNA polymerase II (Rpb1 CTD) levels in the promoters of *Psma6*, *Psmb3*, *Psmb4*, *Psmb6*, and *Actb* genes in the livers of *Mettl3*$^{flox/flox}$ and *Mettl3*-HKO mice at 8 weeks old (n = 5 mice for each group; *Psma6*, $p = 0.0256$; *Psmb3*, $p = 0.027$; *Psmb4*, $p = 0.0024$; *Psmb6*, $p = 0.0033$; *Actb*, $p = 0.3224$; Student's *t* tests). Differences between two groups were analysed using Student's *t* tests. $^{*}p < 0.05$. $^{**}p < 0.01$. Data represent the mean ± SEM. ACTD, actinomycin D; ATAC-seq, assay for transposase-accessible chromatin with sequencing; *Mettl3*-HKO, hepatocyte-specific *Mettl3* knockout; METTL3, methyltransferase-like 3; RNA-seq, RNA sequencing; RT-PCR, real-time PCR; RT-qPCR, real-time quantitative PCR; WT, wild-type.

of liver injury, and the initial GSH depletion reflects the amount of excessive NAPQI generated in the liver. Hepatic deletion of *Mettl3* does not affect either expression of CYP2E1 or the initial depletion of GSH levels during APAP-induced liver injury, which suggests that hepatocyte METTL3 is dispensable for APAP metabolism. However, *Mettl3*-HKO mice show higher basal hepatic GSH levels and faster recovery of hepatic GSH levels at later time points during APAP-induced liver injury, which indicates that METTL3 negatively regulates hepatic GSH levels and higher GSH levels in *Mettl3*-HKO mice are unlikely to contribute to severe APAP-induced liver injury in *Mettl3*-HKO mice. Although proteasome activity is decreased in *Mettl3*-HKO livers, inhibition of proteasome activity does not increase GSH levels. METTL3 regulates hepatic GSH levels likely because of changed expression of GSH metabolism-related genes. Mitochondrial dysfunction and oxidative stress in the liver are similar between *Mettl3*-HKO and *Mettl3*$^{flox/flox}$ mice after APAP treatment, indicating that they are less likely to contribute to more severe APAP-induced liver injury in *Mettl3*-HKO mice.

The activation of the JNK signalling pathway is a key mediator of the pathophysiology of APAP-induced liver injury in both mice and humans. *Mettl3*-HKO mice display enhanced activation and expression of MKK4 and JNK in their livers before and after APAP treatment, which leads to much more severe APAP-induced liver injury. Interestingly, inhibition of JNK by its specific inhibitor (SP600125) completely blocks APAP-induced

liver injury in *Mettl3*-HKO mice. These results indicate that hepatic deficiency of *Mettl3* leads to more severe APAP-induced liver injury as a result of enhanced activation and expression of MKK4 and JNK.

Our focus was on the question of how METTL3 deficiency in hepatocytes causes the activation and expression of MKK4 and JNK. MKK4 and JNK1/2 protein but not mRNA levels are increased, which is because of increased protein stability but not translational efficiency. RNA-seq and RT-qPCR identify many downregulated genes (including *Psmb4* and *Psmb6*) associated with proteasome in *Mettl3*-HKO mice. Consistently, proteasome activity is decreased in *Mettl3*-HKO mice. Restoration of proteasome activity by overexpression of PSMB4 or PSMB6 in *Mettl3*-HKO hepatocytes decreases MKK4 and JNK1/2 protein levels. Interestingly, proteasome activity and the PSMB4/PSMB6 protein levels are also significantly decreased in APAP-induced liver injury. These results indicate that downregulation of proteasome activity and PSMB4/PSMB6 protein levels in APAP-induced liver injury is likely attributable to decreased METTL3 expression, which further contributes to the increased protein stability and activation of MKK4 and JNK. In addition to MKK4 and JNK, p-ERK and ERK levels are also upregulated in *Mettl3*-HKO livers, while p-p38 and p38 levels remain unchanged. These results indicate that METTL3 regulates both the MKK4/JNK and ERK signalling pathways. Whether they share the same molecular mechanisms needs further study.

METTL3 directly regulates APAP-induced hepatocyte death. Overexpression of METTL3 decreases MKK4 and JNK protein levels by upregulating PSMB4 and PSMB6, which protects hepatocytes from APAP-induced hepatocyte death. Conversely, knockdown of *Mettl3* increases MKK4 and JNK protein levels by downregulating PSMB4 and PSMB6 protein levels, which promotes APAP-induced hepatocyte death. Overexpression of METTL3 reverses APAP-induced cell death in *Mettl3* knockdown Hepa1-6 cells. These results indicate that METTL3 negatively regulates MKK4 and JNK protein levels by upregulating PSMB4 and PSMB6, which protects hepatocytes from APAP-induced hepatocyte death.

METTL3 is considered a key RNA methyltransferase that catalyses m^6A mRNA modification and regulates most of the RNA processing steps.[40] Hepatocyte-specific deletion of *Mettl3* largely changes the gene expression profile.[29] Some of the changes depend on m^6A modification, whereas other changes rely on chromatin accessibility independent of m^6A modification.[29] Although genes with downregulated m^6A peaks include *Psmb4* and *Psmb6*, the mRNA stability and translational efficiency of *Psmb4* and *Psmb6* do not change. Instead, the chromatin accessibility is decreased in the promoters of *Psmb4* and *Psmb6*. Consistently, the binding of RNA polymerase II with genes of *Psmb4* and *Psmb6* is decreased in the livers of *Mettl3*-HKO mice. Mechanistically, METTL3 interacts with RNA polymerase II and active histone modifications such as H3K9ac, H3K27ac, and H3K36me3. It also has been shown that METTL14 regulates gene expression by binding to RNA polymerase II and H3K36me3.[39] We and others have also shown that METTL3 and WTAP can bind to gene promoters and regulate gene transcription through different mechanisms.[29,30,41] These results indicate that METTL3 is required for maintaining expression of proteasome components (such as PSMB4 and PSMB6) by binding to RNA polymerase II and active histone modifications such as H3K9ac, H3K27ac, and H3K36me3.

In conclusion, we have shown that hepatic METTL3 is downregulated in APAP-induced liver injury, which promotes APAP-induced liver injury. Hepatocyte-specific deletion of *Mettl3* promotes APAP-induced liver injury, leading to increased mortality, which is most likely as a result of decreased proteasome activity and increased protein stability of MKK4 and JNK, leading to enhanced JNK activation. Inhibition of JNK by SP600125 completely blocks APAP-induced liver injury in *Mettl3*-HKO mice. Therefore, downregulation of *Mettl3* exacerbates APAP-induced liver injury through enhancing the MKK4/JNK signalling pathway with involvement of the decreased proteasome activity.

Abbreviations

ALT, alanine aminotransferase; APAP, acetaminophen; ASK1, apoptosis signal-regulating kinase 1; AST, aspartate transferase; ATAC-seq, assay for transposase-accessible chromatin with sequencing; CYP2E1, cytochrome P-450 2E1; Cytc, cytochrome c; GEO, Gene Expression Omnibus; GSH, glutathione; GSK-3β, glycogen synthase kinase-3 beta; HIT/IACUC, Institutional Animal Care and Use Committee of Harbin Institute of Technology; KEGG, Kyoto Encyclopedia of Genes and Genomes; m^6A, N6-methyladenosine; MAP, mitogen-activated protein; *Mettl3*-HKO, hepatocyte-specific *Mettl3* knockout; METTL3, methyltransferase-like 3; MKP1, MAP kinase phosphatase 1; MLK3, mixed-lineage kinase 3; NAPQI, *N*-acetyl-*p*-benzoquinone imine; PI, propidium iodide; R1P1, receptor interacting protein kinase 1; RNA-seq, RNA sequencing; ROS, reactive oxygen species; RT-PCR, real-time PCR; RT-qPCR, real-time quantitative PCR; WT, wild-type.

Financial support

This study was supported by the National Natural Science Foundation of China grant (31971083 and 92057110).

Conflicts of interest

The authors declare no conflict of interest.

Please refer to the accompanying ICMJE disclosure forms for further details.

Authors' contributions

Performed most of animal experiments: CL; Performed cell culture experiments: XL; Collected an immunoblotting data: MG; Performed the translational efficiency experiment: YD; Conceived and designed the project, researched data, and wrote the manuscript: ZC.

Data availability statement

RNA-seq data that support the findings of this study have been deposited in GEO under accession code GSE214371. All other data are available from the authors upon request.

Acknowledgements

We thank Novogene for assistance in the RNA-seq experiment. We thank Professor Yuanchao Xue from the Institute of Biophysics for helping in the translational efficiency experiment.

Supplementary data

Supplementary data to this article can be found online at https://doi.org/10.1016/j.jhepr.2023.100766.

References

Author names in bold designate shared co-first authorship.

[1] Larson AM, Polson J, Fontana RJ, Davern TJ, Lalani E, Hynan LS, et al. Acetaminophen-induced acute liver failure: results of a United States multicenter, prospective study. Hepatology 2005;42:1364–1372.

[2] Wendon J, Cordoba J, Dhawan A, Larsen FS, Manns M, Nevens F, et al. EASL Clinical Practical Guidelines on the management of acute (fulminant) liver failure. J Hepatol 2017;66:1047–1081.

[3] Bernal W, Auzinger G, Dhawan A, Wendon J. Acute liver failure. Lancet 2010;376:190–201.

[4] Jaeschke H, Xie Y, McGill MR. Acetaminophen-induced liver injury: from animal models to humans. J Clin Transl Hepatol 2014;2:153–161.

[5] Lee SS, Buters JT, Pineau T, Fernandez-Salguero P, Gonzalez FJ. Role of CYP2E1 in the hepatotoxicity of acetaminophen. J Biol Chem 1996;271:12063–12067.

[6] Hanawa N, Shinohara M, Saberi B, Gaarde WA, Han D, Kaplowitz N. Role of JNK translocation to mitochondria leading to inhibition of mitochondria bioenergetics in acetaminophen-induced liver injury. J Biol Chem 2008;283:13565–13577.

[7] McGill MR, Sharpe MR, Williams CD, Taha M, Curry SC, Jaeschke H. The mechanism underlying acetaminophen-induced hepatotoxicity in humans and mice involves mitochondrial damage and nuclear DNA fragmentation. J Clin Invest 2012;122:1574–1583.

[8] Han D, Dara L, Win S, Than TA, Yuan L, Abbasi SQ, et al. Regulation of drug-induced liver injury by signal transduction pathways: critical role of mitochondria. Trends Pharmacol Sc 2013;34:243–253.

[9] **Win S**, **Than TA**, Zhang J, Oo C, Min RWM, Kaplowitz N. New insights into the role and mechanism of c-Jun-N-terminal kinase signaling in the pathobiology of liver diseases. Hepatology 2018;67:2013–2024.

[10] Nakagawa H, Maeda S, Hikiba Y, Ohmae T, Shibata W, Yanai A, et al. Deletion of apoptosis signal-regulating kinase 1 attenuates acetaminophen-induced liver injury by inhibiting c-Jun N-terminal kinase activation. Gastroenterology 2008;135:1311–1321.

[11] Shinohara M, Ybanez MD, Win S, Than TA, Jain S, Gaarde WA, et al. Silencing glycogen synthase kinase-3β inhibits acetaminophen hepatotoxicity and attenuates JNK activation and loss of glutamate cysteine ligase and myeloid cell leukemia sequence 1. J Biol Chem 2010;285:8244–8255.

[12] **Sharma M**, **Gadang V**, Jaeschke A. Critical role for mixed-lineage kinase 3 in acetaminophen-induced hepatotoxicity. Mol Pharmacol 2012;82:1001–1007.

[13] **Zhang Y-F**, **He W**, **Zhang C**, Liu X-J, Lu Y, Wang H, et al. Role of receptor interacting protein (RIP)1 on apoptosis-inducing factor-mediated necroptosis during acetaminophen-evoked acute liver failure in mice. Toxicol Lett 2014;225:445–453.

[14] Ramachandran A, McGill MR, Xie Y, Ni H-M, Ding W-X, Jaeschke H. Receptor interacting protein kinase 3 is a critical early mediator of acetaminophen-induced hepatocyte necrosis in mice. Hepatology 2013;58:2099–2108.

[15] Zhang J, Min RWM, Le K, Zhou S, Aghajan M, Than TA, et al. The role of MAP2 kinases and p38 kinase in acute murine liver injury models. Cell Death Dis 2017;8:e2903.

[16] Wancket LM, Meng X, Rogers LK, Liu Y. Mitogen-activated protein kinase phosphatase (Mkp)-1 protects mice against acetaminophen-induced hepatic injury. Toxicol Pathol 2012;40:1095–1105.

[17] Mobasher MA, González-Rodriguez A, Santamaría B, Ramos S, Martín MA, Goya L, et al. Protein tyrosine phosphatase 1B modulates GSK3beta/Nrf2 and IGFIR signaling pathways in acetaminophen-induced hepatotoxicity. Cel Death Dis 2013;4:e626.

[18] Yue Y, Liu J, He C. RNA N^6-methyladenosine methylation in post-transcriptional gene expression regulation. Genes Dev 2015;29:1343–1355.

[19] Fustin JM, Doi M, Yamaguchi Y, Hida H, Nishimura S, Yoshida M, et al. RNA-methylation-dependent RNA processing controls the speed of the circadian clock. Cell 2013;155:793–806.

[20] **Xiang Y**, **Laurent B**, **Hsu CH**, Nachtergaele S, Lu Z, Sheng W, et al. RNA m^6A methylation regulates the ultraviolet-induced DNA damage response. Nature 2017;543:573–576.

[21] **Ma C**, **Chang M**, **Lv H**, Zhang Z-W, Zhang W, He X, et al. RNA m^6A methylation participates in regulation of postnatal development of the mouse cerebellum. Genome Biol 2018;19:68.

[22] Lin Z, Hsu PJ, Xing X, Fang J, Lu Z, Zou Q, et al. Mettl3-/Mettl14-mediated mRNA N^6-methyladenosine modulates murine spermatogenesis. Cell Res 2017;27:1216–1230.

[23] **Xu K**, **Yang Y**, **Feng G-H**, **Sun B-F**, **Chen J-Q**, Li Y-F, et al. Mettl3-mediated m^6A regulates spermatogonial differentiation and meiosis initiation. Cel Res 2017;27:1100–1114.

[24] Chen T, Hao Y-J, Zhang Y, Li M-M, Wang M, Han W, et al. m^6A RNA methylation is regulated by microRNAs and promotes reprogramming to pluripotency. Cell Stem Cell 2015;16:289–301.

[25] **Geula S**, **Moshitch-Moshkovitz S**, **Dominissini D**, **Mansour AA**, Kol N, Salmon-Divon M, et al. Stem cells. m^6A mRNA methylation facilitates resolution of naive pluripotency toward differentiation. Science 2015;347:1002–1006.

[26] He L, Li J, Wang X, Ying Y, Xie H, Yan H, et al. The dual role of N6-methyladenosine modification of RNAs is involved in human cancers. J Cel Mol Med 2018;22:4630–4639.

[27] Wang Y, Gao M, Zhu F, Li X, Yang Y, Yan Q, et al. METTL3 is essential for postnatal development of brown adipose tissue and energy expenditure in mice. Nat Commun 2020;11:1648.

[28] Wang Y, Li X, Liu C, Zhou L, Shi L, Zhang Z, et al. WTAP regulates postnatal development of brown adipose tissue by stabilizing METTL3 in mice. Life Metab 2022;1:270–284.

[29] **Li X**, **Yuan B**, Lu M, Wang Y, Ding N, Liu C, et al. The methyltransferase METTL3 negatively regulates nonalcoholic steatohepatitis (NASH) progression. Nat Commun 2021;12:7213.

[30] **Li X**, **Ding K**, Li X, Yuan B, Wang Y, Yao Z, et al. Deficiency of WTAP in hepatocytes induces lipoatrophy and non-alcoholic steatohepatitis (NASH). Nat Commun 2022;13:4549.

[31] **De Jesus DF**, **Zhang Z**, **Kahraman S**, Brown NK, Chen M, Hu J, et al. m^6A mRNA methylation regulates human β-cell biology in physiological states and in type 2 diabetes. Nat Metabo 2019;1:765–774.

[32] **Li X**, **Jiang Y**, **Sun X**, Wu Y, Chen Z. METTL3 is required for maintaining β-cell function. Metabolism 2021;116:154702.

[33] Wang Y, Sun J, Lin Z, Zhang W, Wang S, Wang W, et al. m^6A mRNA methylation controls functional maturation in neonatal murine β-cells. Diabetes 2020;69:1708–1722.

[34] **Li X**, **Yang Y**, Chen Z. Downregulation of the m^6A reader protein YTHDC1 leads to islet β-cell failure and diabetes. Metabolism 2023;138:155339.

[35] **Li X**, **Yang Y**, Li Z, Wang Y, Qiao J, Chen Z. Deficiency of WTAP in islet beta cells results in beta cell failure and diabetes in mice. Diabetologia 2023;66:1084–1096.

[36] **Ren X**, **Li X**, Jia L, Chen D, Hou H, Rui L, et al. A small-molecule inhibitor of NF-κB-inducing kinase (NIK) protects liver from toxin-induced inflammation, oxidative stress, and injury. FASEB J 2017;31:711–718.

[37] Li X, Jia L, Chen X, Dong Y, Ren X, Dong Y, et al. Islet α-cell inflammation induced by NF-κB inducing kinase (NIK) leads to hypoglycemia, pancreatitis, growth retardation, and postnatal death in mice. Theranostics 2018;8:5960–5971.

[38] Jia L, Jiang Y, Li X, Chen Z. Purβ promotes hepatic glucose production by increasing Adcy6 transcription. Mol Metab 2020;31:85–97.

[39] **Huang H**, **Weng H**, **Zhou K**, **Wu T**, **Zhao BS**, Sun M, et al. Histone H3 trimethylation at lysine 36 guides m^6A RNA modification co-transcriptionally. Nature 2019;567:414–419.

[40] **Liu J**, **Yue Y**, Han D, Wang X, Fu Y, Zhang L, et al. A METTL3–METTL14 complex mediates mammalian nuclear RNA N^6-adenosine methylation. Nat Chem Biol 2014;10:93–95.

[41] **Barbieri I**, **Tzelepis K**, **Pandolfini L**, Shi J, Millán-Zambrano G, Robson SC, et al. Promoter-bound METTL3 maintains myeloid leukaemia by m^6A-dependent translation control. Nature 2017;552:126–131.